JOURNAL OF GEOPHYSICAL RESEARCH, VOL. 113, D12107, doi:10.1029/2007JD009725, 2008

Production of cosmogenic ^{7}Be isotope in the atmosphere: Full 3-D modeling

Ilya G. Usoskin[1] and Gennady A. Kovaltsov[2]

Received 18 December 2007; revised 11 February 2008; accepted 22 February 2008; published 21 June 2008.

[1] We present a physical model to calculate production of cosmogenic isotope ^{7}Be in the atmosphere. The model is based on a full Monte Carlo simulation of an electromagnetic-muon-nucleonic cascade in the atmosphere, using CORSIKA and FLUKA packages. The present results are in broad agreement with earlier empirical and semiempirical models but predict higher production rate than some recent theoretical models. A comparison to direct and indirect measurements of the ^{7}Be production rate in the atmosphere confirms the validity of the model in the whole range of geographical latitudes and altitudes. Results of the full Monte Carlo simulation are tabulated in a form of the yield function. These tables are given together with a detailed recipe, which allows a user to compute easily the isotope production for given location, altitude, and the spectrum of cosmic rays. An effect of a severe solar energetic particle event of January 2005 is estimated, providing a new tool for tracing of mass transport.

Citation: Usoskin, I. G., and G. A. Kovaltsov (2008), Production of cosmogenic ^{7}Be isotope in the atmosphere: Full 3-D modeling, *J. Geophys. Res.*, *113*, D12107, doi:10.1029/2007JD009725.

1. Introduction

[2] Cosmogenic isotopes with a relatively short lifetime have been long recognized as useful tools to study atmospheric transport of air masses [e.g., *Lal and Peters*, 1962; *Raisbeck et al.*, 1981]. Particularly suitable for this purpose is the cosmogenic isotope ^{7}Be (the half-life time of 53.6 days), which is produced through interactions of atmospheric O and N nuclei and the nucleonic component of the atmospheric cascade induced by galactic cosmic rays (GCR) [see, e.g., *Dorman*, 2004, chapter 10.6]. Shortly after formation ^{7}Be atoms become attached to atmospheric aerosols and thus their fate is related to the aerosol transport. Therefore, ^{7}Be appears to be an excellent tracer for the atmospheric circulation, and is often used to constraint atmospheric circulation models [e.g., *Koch et al.*, 1996; *Liu et al.*, 2001; *Jordan et al.*, 2003], when the data on measurements of the isotope concentration in stratospheric or tropospheric air is confronted with predictions of modern sophisticated 3-D models of the air mass transport.

[3] For this purpose one needs to know precisely features of its production in the atmosphere, including altitude and latitude profiles. A number of models have been developed to compute the ^{7}Be production in the atmosphere, as presented in Table 1. The first consistent model was developed by D. Lal and coworkers [*Bhandari et al.*, 1966; *Lal and Peters*, 1967; *Lal and Suess*, 1968], called henceforth LP67. The LP67 model uses an empirical approach based on fitting simplified model calculations to measurements of the isotope concentrations and "star" (inelastic nuclear collisions) formations in the atmosphere. Accordingly, the LP67 model yields the best agreement with measurements of stratospheric ^{7}Be (see discussion by *Liu et al.* [2001]). Next was an analytical model by *O'Brien* [1979] (hereinafter referred to as OB79), who solved the problem of GCR-induced cascade in the atmosphere using an analytical stationary approximation in the form of Boltzman equation, which has been also normalized per "star" formation. Those models were based on calculating the rate of inelastic collisions or "stars" and then applied the mean spallation yield per "star." This approach has been further developed by *Nagai et al.* [2000] (called N00 henceforth) who calculated the isotope production using secondary neutron spectra obtained by *Armstrong et al.* [1973] for the solar activity minimum conditions, and recent cross sections instead of the mean yield of a "star." The N00 model is semiempirical and contains essential simplifications; for example, its proton spectrum was obtained by scaling from neutron spectra and applied in the same shape to all depths. Moreover, it is valid only for the solar minimum conditions. A new step in modeling of the isotope production has been made by *Masarik and Beer* [1999] (hereinafter referred to as MB99), who performed a full Monte Carlo simulation of the GCR-initiated cascade of the atmosphere and directly used cross sections of spallation reactions instead of the average "star" efficiency. Since *Masarik and Beer* [1999] were interested in the total production rather than in its altitude profile, they used an approximation of the flat atmosphere. The models described above compute isotope production by galactic cosmic rays and do not consider production by solar energetic particles (SEP). A recent model by *Webber and Higbie* [2003] and

[1]Oulu Unit, Sodankylä Geophysical Observatory, University of Oulu, Oulu, Finland.
[2]Ioffe Physical-Technical Institute, St. Petersburg, Russia.

0148-0227/08/2007JD009725$09.00

Table 1. Comparison of the Parameters of Models for ^{7}Be Production in the Atmosphere[a]

Model	LP67	OB79	MB99	N00	WH03/07	This Model
Method	empirical	analytical	MC[b] GEANT	Semiempirical	MC[b] FLUKA	MC[b] CORSIKA
Atmosphere	N/A[c]	spherical shell	flat	N/A	flat	realistic curved
CR flux	N/A	isotropic flux	isotropic flux	N/A	vertical beam	isotropic flux
Heavier CR	N/A	α, scaling	α, scaling	N/A	scaling	α, explicitly
Altitude profiles	yes	N/A	N/A	yes	N/A	yes
Latitude profiles	yes	N/A	yes	yes	yes	yes
Production function	no	no	no	no	yes	yes
CR type	GCR	GCR	GCR	GCR, solar min	GCR + SEP	GCR + SEP
Global production[d]	0.08	0.063	0.035	0.055–0.062[e]	0.035[f]	0.062[g]

[a]LP67 [*Lal and Peters*, 1967; *Lal and Suess*, 1968], OB79 [*O'Brien*, 1979; *O'Brien et al.*, 1991], MB99 [*Masarik and Beer*, 1999], N00 [*Nagai et al.*, 2000], and WH03/07 [*Webber and Higbie*, 2003; *Webber et al.*, 2007], as well as the present model.
[b]Monte Carlo simulations.
[c]Not available (N/A).
[d]Global production (in atoms cm^{-2} s^{-1}), averaged over a solar cycle.
[e]The value 0.068 (atoms cm^{-2} s^{-1}) originally given for the solar activity minimum has been reduced by 10–20% for the averaged solar cycle [*Nagai et al.*, 2000].
[f]W. R. Webber (personal communication, 2007).
[g]Calculated for ϕ = 0.7 GV and geomagnetic field for the epoch 2005.

Webber et al. [2007] (hereinafter referred to as WH03/07) is also based on a full Monte Carlo simulation of the atmospheric cascade. The WH03/07 model uses improved cross sections and is advanced with respect to MB99 in the sense that it first computes the yield function (see section 2.4) for a fixed energy of GCR. This approach allows much more flexibility with the model application, in particular computing an effect of SEP, whose energy spectrum is totally different from that of GCR (see section 4). However, the WH03/07 model is simplified in the sense that it assumes a flat atmosphere and a vertical beam of primary GCR particles. With little effect on the total ^{7}Be production, this assumption is crucial for the results in the stratosphere. Main properties of the earlier models have been summarized in Table 1. It is important to mention that most of the earlier models do not provide information on the altitudinal profiles of the isotope production and are not able to deal with the effect of solar energetic particles, which, as argued in section 4, can be quite important for a severe SEP event.

[4] Accordingly, there is a need for a calibrated model that is able to compute a full 3-D pattern of the ^{7}Be production in the atmosphere, including detailed simulation of the SEP effect. Here we present such a model, which can compute production of ^{7}Be isotope in the atmosphere, including altitude and geographical profiles. Flexibility of the model allows a direct computation of the effect of SEP or other transient events. A special emphasis is given to comparison of the present model results with direct and indirect measurements and with other models. We provide a full numerical recipe so that everyone interested can compute the ^{7}Be production in any prescribed solar and geophysical conditions.

2. Modeling the Isotope Production in the Atmosphere

2.1. Monte Carlo Simulations of the Atmospheric Cascade

[5] The isotope ^{7}Be is produced in the atmosphere mainly as a result of spallation of oxygen and nitrogen by energetic protons, neutrons and α nuclei. These energetic particles can be either primary cosmic rays in the upper atmosphere or secondary nucleonic components of the cascade initiated by interactions of cosmic rays in the atmosphere. We have modeled development of the atmospheric cascade by means of a Monte Carlo simulation tool CORSIKA (Cosmic Ray Simulations for Kascade, version 6.617, August 2007) [*Heck et al.*, 1998]. Interactions between low-energy (below 80 GeV of total energy) hadrons were treated with the FLUKA tool (version 2006.3b, March 2007) [*Fassò et al.*, 2001]. We used a realistic curved atmosphere, in contrast to flat atmospheres used in most earlier models, also allowing for upward moving secondary particles. Using the curved atmosphere is important for the stratosphere. The chemical composition of the atmosphere was taken as N_2, O_2 and Ar in the volume fractions of 78.1%, 21% and 0.9%, respectively. The atmosphere's density profile was modeled according to the standard U.S. atmosphere parameterized by *Keilhauer et al.* [2004].

[6] The flux of primary cosmic rays corresponding to their CR intensity with isotropic angular distribution, J given in (cm^2 s sr GeV)$^{-1}$, has been modeled as follows. The corresponding particle flux, F in (cm^2 s GeV)$^{-1}$, impinging on the top of the atmosphere is defined as [see, e.g., *Grieder*, 2001, equation (1.35)]

$$F = 2\pi \int_0^1 J \ \cos\theta \ d(\cos\theta), \tag{1}$$

where θ is the incident zenith angle. We note that the unit flux, i.e., F = 1, corresponds to the CR intensity $J = 1/\pi$. Therefore, the distribution (over the zenith angle θ) of the primary CR particles impinging on the atmosphere is proportional to cos θ:

$$\frac{dF}{d\cos\theta} = 2\cos\theta, \tag{2}$$

for the unit flux. Accordingly, when simulating the cascade, we threw primary CR particles with a fixed kinetic energy on the top of the atmosphere with the zenith angle distribution proportional to cosine of the zenith angle (equation (2)) and with the even azimuthal distribution. Cascade simulations have been done separately for two

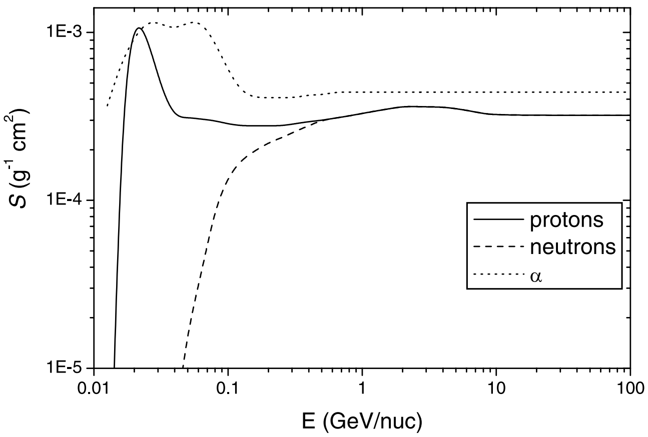

Figure 1. Efficiency of ^{7}Be production in air (see text).

types of primary cosmic rays, protons and α particles. The number of simulated cascades N was chosen depending on the energy of primary CR particle E_o so that the statistical uncertainty of the final result is below 1%, which is much better than uncertainties in the used cross sections. We have performed $3 \cdot 10^6$ cascade simulation runs for each fixed value of E_o below 1 GeV/nucleon, 10^6 runs for $1 \leq E_o <$ 10 GeV/nucleon, $3 \cdot 10^5$ runs for $10 \leq E_o <$ 100 GeV/nucleon, and 10^5 runs for higher energies.

[7] For each cascade simulation we have fixed all the secondary and primary particles of the following types (protons p, neutrons n and α particles) that cross a fixed observation level h in the atmosphere. For each such particle we have recorded three components of its momentum, P_x, P_y, P_z, in the Cartesian coordinate system with the z axis pointing to nadir. Then the angle ψ between the nadir and the direction of the particle's momentum is defined as

$$\cos\psi = \frac{P_z}{\sqrt{P_x^2 + P_y^2 + P_z^2}} \tag{3}$$

[8] This information has been collected over all simulation runs with a given energy E_o of primary CR particles and for fixed atmospheric depth h, and used in forthcoming computations.

2.2. Isotope Production Function

[9] Since the development of atmospheric cascade is defined mostly by the amount of matter traversed, we express altitude in units of the atmospheric depth, i.e., the amount of the atmospheric matter in g/cm^2 overburden at a given level in the atmosphere. It is directly related to the barometric pressure so that the sea level (1013 mbar barometric pressure) corresponds to the atmospheric depth of 1033 g/cm^2. Average (per one primary particle of type A with energy E_o) production of ^{7}Be, in units of atoms g^{-1} cm^2, at the atmospheric depth h can be defined as a sum of productions by all secondaries

$$\frac{dq}{dh}(E_o, h, A) = \frac{1}{N(E_o)}\left(\sum\nolimits_i \frac{Sp(E_i)}{|\cos\psi_i|} + \sum\nolimits_j \frac{Sn(E_j)}{|\cos\psi_j|} + \sum\nolimits_k \frac{S\alpha(E_k)}{|\cos\psi_k|}\right), \tag{4}$$

where $N(E_o)$ is the number of the simulated cascades with the primary particle's energy E_o and type A (protons or α particles), and the three items correspond to sums over all secondary protons, neutrons and α particles, respectively, recorded as crossing the observational level h. Numerators of the sums represent the efficiency of the isotope production in air by a particle (p, n or α) with the kinetic energy E:

$$\begin{aligned} Sp(E) &= \kappa_O \cdot \sigma_{pO}(E) + \kappa_N \cdot \sigma_{pN}(E), \\ Sn(E) &= \kappa_O \cdot \sigma_{nO}(E) + \kappa_N \cdot \sigma_{nN}(E), \\ S\alpha(E) &= \kappa_O \cdot \sigma_{\alpha O}(E) + \kappa_N \cdot \sigma_{\alpha N}(E), \end{aligned} \tag{5}$$

where σ_{xY} is the cross section of ^{7}Be production by particle of type x on target Y, $\kappa_O = 8.672 \cdot 10^{21}$ g^{-1} and $\kappa_N = 3.225 \cdot 10^{22}$ g^{-1} are the numbers of oxygen and nitrogen nuclei, respectively, in gram of air. Cross sections have been adopted from *Lange et al.* [1994], *Tatischeff et al.* [2006], *Webber and Higbie* [2003], and *Webber et al.* [2007]. The resultant efficiency curves are shown in Figure 1.

2.3. Production in the Upper Atmosphere

[10] The CORSIKA code is not well suited for simulations of the upper atmosphere ($h \leq 10$ g/cm^2) before the first nuclear interaction. Therefore, we have also performed an analytical calculation of the ^{7}Be production in the upper 10 g/cm^2 atmospheric layer, using a thin target approximation. In this thin layer, secondaries can be neglected, and the isotope is produced by reactions between primary CR particles and the target nuclei. Let us consider a primary proton with energy E_o penetrating to the atmosphere at zenith angle θ. We neglect elastic scattering and assume that the particle moves straight, but loses its energy due to ionization of the ambient air or is lost due to nuclear inelastic processes. The probability of a particle of type A with initial energy Eo to survive, against inelastic process, until its energy becomes E' is given as

$$W(E_o, E', A) = \exp\left(-\int_{E'}^{E_o} \frac{dE}{\frac{dE}{dx}(E,A) \cdot \lambda_{in}(E,A)}\right), \tag{6}$$

where $\frac{dE}{dx}(E, A)$ and $\lambda_{in}(E, A)$ are the stopping power due to ionization losses and the path length for inelastic nuclear collisions, respectively, as tabulated by *Janni* [1982]. The energy E' is related to the distance x traversed by the particle along its trajectory as

$$x = R(E_o) - R(E'), \tag{7}$$

where $R(E)$ is the path length of a particle with energy E due to ionization losses [*Janni*, 1982]. Then the isotope production at a distance x is given as

$$\frac{dq}{dx}(x, E_o, A) = S_A(E') \cdot W(E_o, E', A), \tag{8}$$

where S_A is taken from equation (5) and E' is defined from the equation (7).

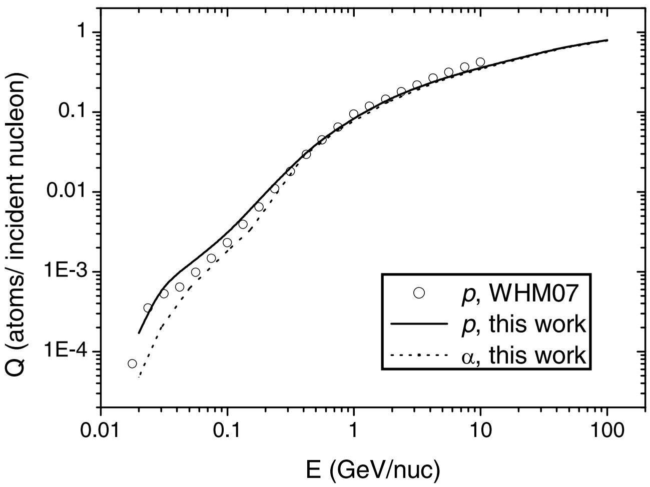

Figure 2. Total production of ^{7}Be in the atmosphere as function of the energy of primary cosmic ray particle. Solid and dotted curves depict the results of this work for primary protons and α particles (the latter is shown per nucleon). Open circles correspond to the computations by *Webber and Higbie* [2003] for primary protons.

[11] For a particle with the incident zenith angle θ, the relation between the distance traversed by the particle x and the atmospheric depth h is

$$x = \frac{h}{\cos\theta} \tag{9}$$

[12] The above consideration was derived for a single primary particle with energy E_o entering the atmosphere at the zenith angle θ. Assuming isotropically impinging particles and a flat atmosphere, one can obtain the expected isotope production in a thin upper layer dh

$$\frac{dq}{dh}(h, E_o, A) = \int_0^1 \frac{dq}{dx} \cdot \frac{dx}{dh} \cdot \frac{dF}{d(\cos\theta)} \cdot d\cos\theta = 2\int_0^1 \frac{dq}{dx} \cdot d\cos\theta \tag{10}$$

[13] Note that at the top of the atmosphere (h = 0) this integral is reduced to

$$\frac{dq}{dh}(E_o, h = 0, A) = 2S_{\mathrm{A}}(E_o) \tag{11}$$

[14] The results obtained by CORSIKA appear quite close to the analytical approximation, described above, for the atmospheric depth h between 0 and 20 g/cm^2 (altitude above 25 km). For the atmospheric layers above h = 10 g/cm^2 (about 30 km) we used the analytical results of ^{7}Be production (equation (11)).

2.4. Yield Function

[15] The column production of ^{7}Be in the atmosphere by one primary particle of type A with energy E_o is an integral over the entire atmospheric column

$$q(E_o) = \int_0^{h_{\mathrm{s.l.}}} \frac{dq}{dh}\, dh, \tag{12}$$

where $h_{\mathrm{s.l.}}$ = 1033 g/cm^2 is the atmospheric depth at the sea level. The dependence of q on the primary particle's energy is shown in Figure 2 for primary protons and α particles. For comparison, a similar result of the WH03/07 model for primary protons is also shown. The overall agreement is quite good, taking into account the different models used.

[16] However, since we are interested in both the total production and in its altitudinal profile, we present here a concept of the yield function of ^{7}Be at a given atmospheric depth. The yield function is defined as the production of the isotope by primary particles of type A with the unit intensity J (i.e., one primary particle with energy E_o in the interplanetary space per steradian per second per cm^2) and is related to the production function dq/dh (which is the isotope production per unit flux F, i.e., one particle crossing a horizontal 1 cm^2 area at the top of the atmosphere per second) as

$$Y(E_o, h, A) = \pi \frac{dq}{dh}(E_o, h, A), \tag{13}$$

where the units of Y are atoms g^{-1} cm^2 sr. The factor π appears as conversion between the flux on the top of the atmosphere and CR intensity in the interplanetary space (see equation (1)).

[17] The tabulated yield function is presented in Tables 2 and 3 for primary cosmic protons and α particles, respectively. Throughout the paper we discuss the isotope production per nucleon of the incident primary particle; that is, the production by one α particle is four times that shown here.

[18] As an additional test for the correctness of our computations of the nucleonic component of the cascade and the yield function, we computed the yield function of a standard NM64 sea-level neutron monitor in a way similar to equation (13), but using the NM64 efficiency S_{NM64} [*Hatton*, 1971; *Clem and Dorman*, 2000] instead of the ^{7}Be production efficiency (equation (5)). A ground-based neutron monitor detects, with the known efficiency, superthermal secondary neutrons which are also the main source of the ^{7}Be isotope in the troposphere. The neutron monitor yield function has been thoroughly studied earlier by different groups and methods, including Monte Carlo simulations and confronting the obtained results with direct measurements in a wide range of conditions [see *Clem and Dorman*, 2000; and references therein]. Thus computed NM yield function is shown in Figure 3 together with the yield function computed by *Clem and Dorman* [2000], and one can see a close agreement between them, including both the shape and the absolute values. This confirms correctness of our computations of the flux of secondary neutrons in our approach.

2.5. Galactic Cosmic Rays Spectrum

[19] The spectrum of GCR at the Earth's orbit is often parameterized by the so-called force field model [*Gleeson and Axford*, 1968; *Caballero-Lopez and Moraal*, 2004], where the spectrum of ith specie (with the charge number Z_i and the mass number A_i) of CR at Earth's orbit, J_i, is related to an unmodulated local interstellar spectrum (LIS)

Table 2. Normalized Yield Function Y_p/π of ^{7}Be Production by Primary Cosmic Protons[a]

h/E_0	0.02	0.03	0.05	0.1	0.15	0.4	0.76	1.9	4.6	10.0	21.5	46.4	100
0	2.6E-3	1.1E-3	6.2E-4	5.6E-4	5.6E-4	6.0E-4	6.0E-4	6.0E-4	6.0E-4	6.0E-4	6.0E-4	6.0E-4	6.0E-4
10	0	1.0E-10	4.0E-6	1.4E-4	2.4E-4	5.0E-4	6.3E-4	7.0E-4	8.5E-4	9.0E-4	9.5E-4	9.9E-4	1.0E-3
20	0	0	0	0	7.4E-5	4.5E-4	6.5E-4	7.6E-4	9.2E-4	1.1E-3	1.2E-3	1.2E-3	1.3E-3
45	0	0	0	0	6.8E-6	2.9E-4	4.8E-4	7.3E-4	9.4E-4	1.2E-3	1.4E-3	1.6E-3	1.5E-3
100	0	0	0	0	9.7E-7	6.2E-5	2.2E-4	5.4E-4	8.5E-4	1.2E-3	1.4E-3	1.8E-3	2.0E-3
200	0	0	0	0	2.3E-7	1.3E-5	6.5E-5	2.9E-4	5.6E-4	8.4E-4	1.1E-3	1.6E-3	1.8E-3
300	0	0	0	0	7.0E-8	5.0E-6	2.5E-5	1.5E-4	3.3E-4	5.3E-4	7.5E-4	1.1E-3	1.4E-3
400	0	0	0	0	1.0E-8	2.0E-6	1.0E-5	6.4E-5	1.8E-4	2.9E-4	4.6E-4	7.0E-4	9.3E-4
500	0	0	0	0	0	7.5E-7	4.0E-6	2.7E-5	9.0E-5	1.5E-4	2.5E-4	4.0E-4	5.8E-4
700	0	0	0	0	0	1.9E-7	8.6E-7	5.8E-6	2.4E-5	4.3E-5	7.6E-5	1.3E-4	2.0E-4
850	0	0	0	0	0	1.1E-7	3.6E-7	2.2E-6	8.0E-6	1.7E-5	3.0E-5	5.5E-5	8.0E-5
1000	0	0	0	0	0	7.6E-8	2.1E-7	8.5E-7	3.2E-6	6.1E-6	1.1E-5	2.1E-5	3.5E-5

[a]Unit of ^{7}Be production is atoms g^{-1} cm^2. Column 1 depicts the atmospheric depth h in g/cm^2. Columns 2–14 depict the energy in GeV/nucleon.

of the same specie, $J_{\mathrm{LIS},i}$ via the modulation potential ϕ (given in GV) as:

$$J_i(T,\phi) = J_{\mathrm{LIS},i}(T+\Phi_i)\frac{(T)(T+2T_\mathrm{r})}{(T+\Phi_i)(T+\Phi_i+2T_\mathrm{r})}, \tag{14}$$

where T is the particle's kinetic energy per nucleon, $\Phi_i = (eZ_i/A_i)\phi$, and T_r is the proton's rest energy. The modulation potential provides a good single-parameter approximation of the observed shape of the CR spectrum near Earth [e.g., *Usoskin et al.*, 2005]. The value of ϕ varies between about 0.4 GV (solar minimum) and 1.2 GV (solar maximum) but may reach up to 2 GV during strong transient GCR suppressions, such as Forbush decreases. An implicit parameter of the force field approximation is the shape of the LIS, which is not well known. Here we use the LIS for protons according to *Burger et al.* [2000] in parameterizations by *Usoskin et al.* [2005]

$$J_{\mathrm{LIS},p}(T) = \frac{1.9\cdot P(T)^{-2.78}}{1+0.4866\,P(T)^{-2.51}}, \tag{15}$$

where J is expressed in units of nucleons/(cm^2 sr s GeV/nucleon), and

$$P(T) = \sqrt{T(T+2\cdot T_\mathrm{r})}, \tag{16}$$

where T is given in GeV/nucleon, and T_r = 0.938 GeV/nucleon. As an example, Figure 4 shows the daily fluence of galactic protons for solar maximum and minimum. The solar cycle variations of the lower part of the spectrum are as large as an order of magnitude.

[20] The LIS of the heavier species has been taken of the same shape as the LIS of protons (equation (15)) but scaled to match the abundance ratios in the interstellar space in high energy [*Alcaraz et al.*, 2000; *Usoskin et al.*, 2005]. Note that the Z_i/A_i ratio for α particles is half of that for hydrogen with the same energy per nucleon, hence the fraction of α particles in the overall CR flux near Earth is increasing with decreasing particle's energy and increasing modulation potential (see equation (14)). Since the heavier species are approximately identical to α particles in the sense of the heliospheric modulation ($Z_i/A_i \approx 1/2$) as well as in the ^{7}Be production, we consider all the nuclei, heavier than protons, as α particles with the corresponding number of nucleons. The nucleonic ratio of heavier nuclei (including α particles) to protons is chosen to be 0.3 in the interstellar space [e.g., *Gaisser and Stanev*, 2004], i.e. (compare equation (15)),

$$J_{\mathrm{LIS},\alpha}(T) = \frac{0.57\cdot P(T)^{-2.78}}{1+0.4866\,P(T)^{-2.51}}, \tag{17}$$

where P is defined by equation (16).

2.6. Final Step in Computing the Isotope Production

[21] Production of ^{7}Be can be computed using the yield function in a way similar to computation of the cosmic ray induced ionization in the atmosphere [*Usoskin and Kovaltsov*, 2006].

Table 3. Normalized Yield Function Y_α/π ^{7}Be Production by Primary Cosmic α Particles[a]

h/E_0	0.02	0.03	0.05	0.1	0.15	0.4	0.76	1.9	4.6	10.0	21.5	46.4	100
1	5.0E-4	5.5E-4	6.0E-4	3.0E-4	2.0E-4	2.0E-4	2.3E-4	2.3E-4	2.3E-4	2.3E-4	2.3E-4	2.3E-4	2.3E-4
10	0	0	1.0E-7	1.3E-4	1.9E-4	2.9E-4	3.8E-4	4.8E-4	5.6E-4	6.8E-4	7.6E-4	8.0E-4	8.5E-4
20	0	0	0	0	4.6E-5	3.2E-4	4.1E-4	5.5E-4	7.0E-4	8.5E-4	1.0E-3	1.1E-3	1.2E-3
45	0	0	0	0	5.0E-6	2.3E-4	4.0E-4	6.4E-4	9.0E-4	1.2E-3	1.4E-3	1.6E-3	1.8E-3
100	0	0	0	0	6.0E-7	9.0E-5	2.2E-4	5.0E-4	8.7E-4	1.2E-3	1.5E-3	1.8E-3	2.0E-3
200	0	0	0	0	6.0E-8	2.8E-5	1.1E-4	2.9E-4	5.5E-4	8.2E-4	1.2E-3	1.5E-3	1.8E-3
300	0	0	0	0	0	1.0E-5	4.0E-5	1.5E-4	3.3E-4	5.0E-4	7.5E-4	1.1E-3	1.3E-3
400	0	0	0	0	0	4.5E-6	1.7E-5	6.7E-5	1.7E-4	2.8E-4	4.4E-4	6.6E-4	9.3E-4
500	0	0	0	0	0	1.7E-6	6.5E-6	3.0E-5	9.0E-5	1.5E-4	2.4E-4	3.7E-4	6.0E-4
700	0	0	0	0	0	3.9E-7	1.6E-6	6.7E-6	2.3E-5	4.0E-5	7.1E-5	1.2E-4	2.0E-4
850	0	0	0	0	0	2.0E-7	6.0E-7	2.5E-6	8.0E-6	1.5E-5	2.5E-5	5.0E-5	9.0E-5
1000	0	0	0	0	0	1.4E-7	3.0E-7	1.1E-6	3.0E-6	5.4E-6	9.4E-6	1.8E-5	3.2E-5

[a]Unit of ^{7}Be production is atoms g^{-1} cm^2. Column 1 depicts the atmospheric depth h in g/cm^2. Columns 2–14 depict the energy in GeV/nucleon.

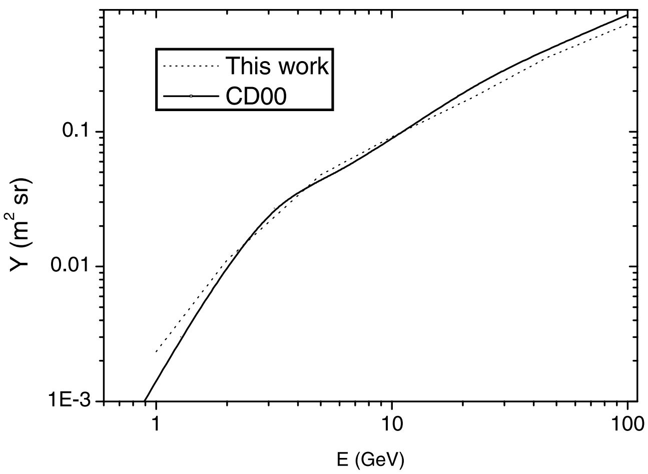

Figure 3. The yield function of a standard NM64 sea-level neutron monitor. Solid and dotted curves present the results from *Clem and Dorman* [2000] and from the present work, respectively.

[22] A product of the yield function Y and spectrum J is the differential production function of ^{7}Be:

$$D(h, E_o, \phi, A) = Y(h, E_o, A) \cdot J(E_o, \phi, A). \quad (18)$$

[23] An example of the production function D for protons is shown in Figure 5, for $\phi = 0.7$ GV and several values of the atmospheric depth. One can see that the most effective energy of cosmic rays for the isotope production depends on the atmospheric depth. The maximum production in the stratosphere is due to particles with an energy of about 1 GeV/nucleon. The peak, corresponding to the effective energy, moves toward higher energies with decreasing altitude, being about 3 GeV/nucleon for lower troposphere. Once the production function $D(E_o, h, A, \phi)$ is known, the production of the isotope at a given atmospheric level h and geomagnetic cutoff rigidity P_c can be computed as a sum (over different species of cosmic rays) of integrals of D over the energy of primary cosmic rays:

$$Q(h, \phi, P_c) = \sum_i Q_i = \sum_i \int_{T_{c,i}}^{\infty} J_i(T, \phi) Y_i(h, T) dT, \quad (19)$$

where Y_i is the yield function and J_i is the differential energy spectrum of the ith specie of GCR (protons and α particles here). Integration is over the kinetic energy above $T_{c,i}$, which is the kinetic energy corresponding to the local vertical geomagnetic rigidity cutoff P_c. This cutoff energy (per nucleon) depends on the Z_i/A_i ratio of the cosmic ray specie and is given as

$$T_{c,i} = T_r \cdot \left(\sqrt{\left(\frac{Z_i \cdot P_c}{A_i \cdot T_r}\right)^2 + 1} - 1 \right). \quad (20)$$

[24] This implies that particles with the ratio of $Z_i/A_i < 1$ are less deflected by the geomagnetic field, which, in combination with their weaker heliospheric modulation, makes them crucially important in the isotope production. Therefore, contribution of heavier species cannot be neglected in realistic models of the isotope production.

[25] We note that using the vertical geomagnetic cutoff P_c does not account for realistic directional geomagnetic cutoffs but it provides a reasonable first-order approximation [e.g., *Cooke*, 1983; *O'Brien*, 2005] to the effective cutoff for isotropically impinging flux. Although this approach is supported by the agreement between our results and the measurements, it may be a source of uncertainties, and detailed computations of cosmic ray transport in the magnetosphere are planned for the future. A question of the

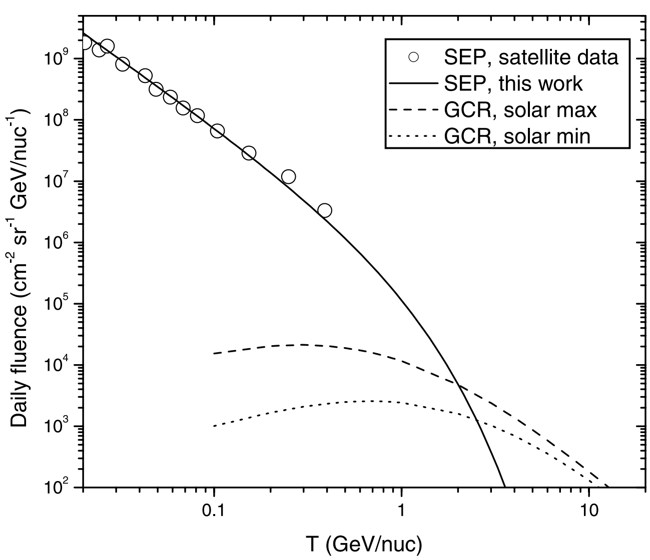

Figure 4. Daily differential energy fluence of cosmic protons. Dashed and dotted curves correspond to galactic protons for the minimum ($\phi = 0.4$ GV) and maximum ($\phi = 1.2$ GV) of solar activity, respectively. The traditional spectrum can be obtained by dividing these values by 86400, the number of seconds in 1 day. Open dots and solid line represent the spaceborne measurements of solar energetic particles [*Mewaldt et al.*, 2005] and our best fit (see equation (21)), respectively.

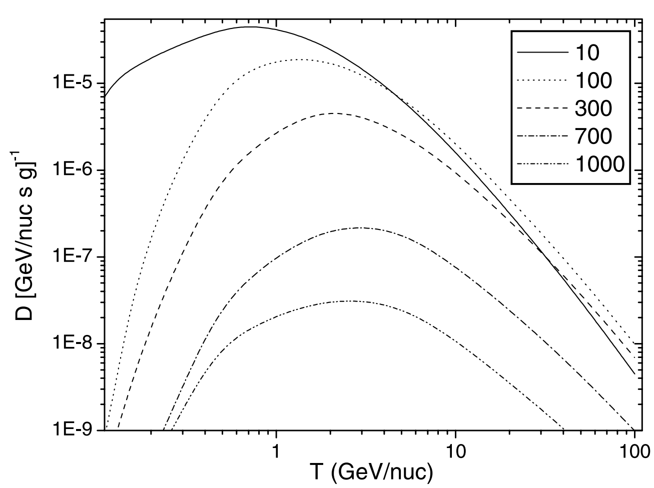

Figure 5. The differential production function D for primary protons at different atmospheric depths as denoted in the legend in units of g/cm^2. The proton spectrum corresponds to $\phi = 0.7$ GV.

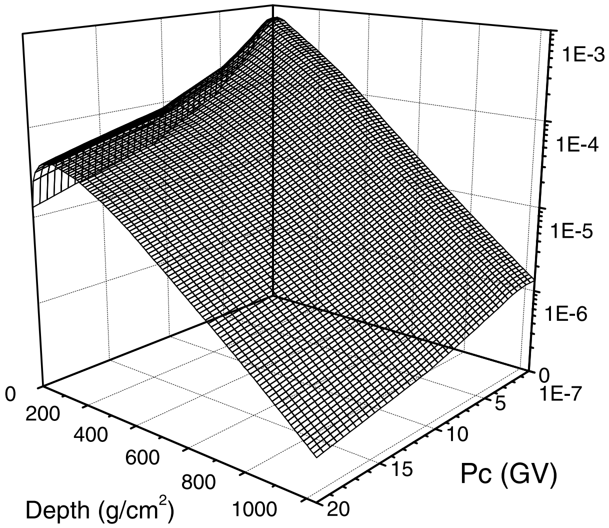

Figure 6. Production rate of ^{7}Be in the atmosphere as function of the atmospheric depth and geomagnetic cutoff rigidity P_c. The modulation potential is fixed at the value ϕ = 0.7 GV, corresponding to a medium modulation of cosmic rays.

precise determination of P_c for a given location and time is a separate problem [*Cooke et al.*, 1991; *Kudela and Bobik*, 2004], which is left beyond the scope of the present study.

2.7. Recipe

[26] By means of the above formalism one can easily compute the ^{7}Be production rate for a given altitude h, location P_c and time (or actually, the modulation potential ϕ), using the following recipe:

[27] 1. Tabulated values of the yield function $Y(E_o, h)/\pi$ are given in Tables 2 and 3 for protons and α particles, respectively.

[28] 2. The value of the modulation potential ϕ can be obtained for a given period from *Usoskin et al.* [2005] or from a continuously updated list at http://cosmicrays.oulu.fi/phi. The shape of the differential energy spectrum $J(T, \phi)$ is then calculated using equations (14)–(17) for both protons and α particles.

[29] 3. The final production rate is computed using equation (19), where the integration bounds are different for the two species of GCR (see equation (20)).

[30] The authors have also computed and tabulated the production rate Q (equation (19)) for a 3-D grid of h (0–1030 g/cm^2 with the grid size of 10 g/cm^2), P_c (0–20 GV with the grid size of 0.5 GV) and ϕ(0–1.5 GV with the grid size of 0.05 GV). These digital tables are available in the auxiliary material[1] or can be requested directly from the authors. The authors would be also happy to provide, upon requests, computation of ^{7}Be production rate for any specific location and/or time, including contribution from solar energetic particles (see section 4).

2.8. Results

[31] The main result of this model is a three-dimensional (h, P_c and ϕ) matrix of the ^{7}Be production rate Q, which can be found in the auxiliary material or requested from the authors. Since a 3-D function cannot be plotted, we show in Figure 6 its 2-D projection for a fixed medium cosmic ray modulation.

[32] One can see that the strongest dependence is over the atmospheric depth (altitude), being two–three orders of magnitude between the maximum at 20–30 km and the minimum at the sea level. Dependence on the geomagnetic cutoff rigidity is moderate, being a factor of 3–20 (depending on the altitude) between geomagnetic poles and equator. The range of production variations due to the 11-year solar cycle is from 15% (sea level at the equator) to a factor of 3 (polar upper stratosphere). Four curves bounding geographical (between the geomagnetic pole and equator) and solar cycle variations of the production rate are shown in Figure 7.

[33] We note that the total or column production (i.e., production within the atmospheric column of unit area) of ^{7}Be is not representative because of the isotope's short lifetime, comparable to or shorter than the residence time. Therefore, a more local production should be considered, especially in the stratosphere. However, for the sake of comparison with other models, we have computed the column production as a function of the geomagnetic latitude as shown in Figure 8. The global average production of ^{7}Be in the atmosphere is evaluated as 0.078 and 0.05 (at cm^{-2} s^{-1}) for the solar minimum (ϕ = 0.4 GV) and maximum (ϕ = 1.2 GV), respectively. The global production for the medium solar activity (ϕ = 0.7 GV) is 0.062 (at cm^{-2} s^{-1}), which can be compared with the results of other models in Table 1. These values are computed for the geomagnetic field, corresponding to the epoch 2005. Keeping in mind that the geomagnetic field strength keeps steadily decreasing

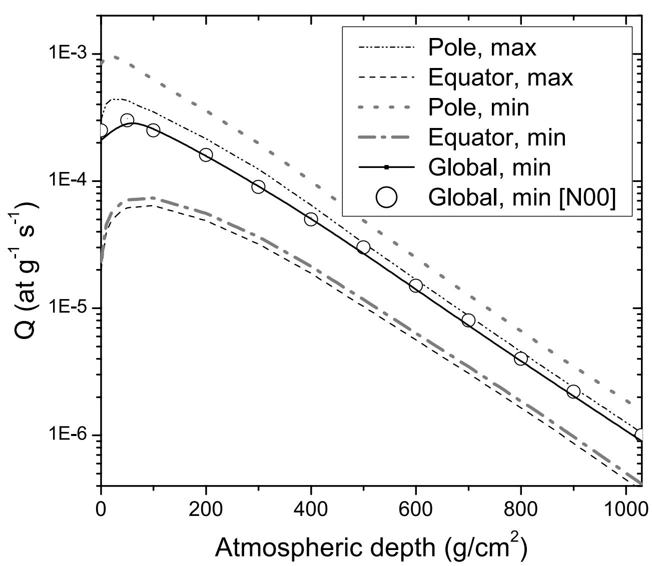

Figure 7. Production rate of ^{7}Be in the atmosphere as a function of the atmospheric depth. Different dashed curves correspond to the geomagnetic pole and equator and to solar cycle minimum (ϕ = 0.4 GV) and maximum (ϕ = 1.2 GV) conditions as denoted in the legend. Solid curve and open circles correspond to the global production for the solar minimum conditions, as results of this model and N00, respectively.

[1]Auxiliary materials are available at ftp://ftp.agu.org/apend/jd/2007jd009725.

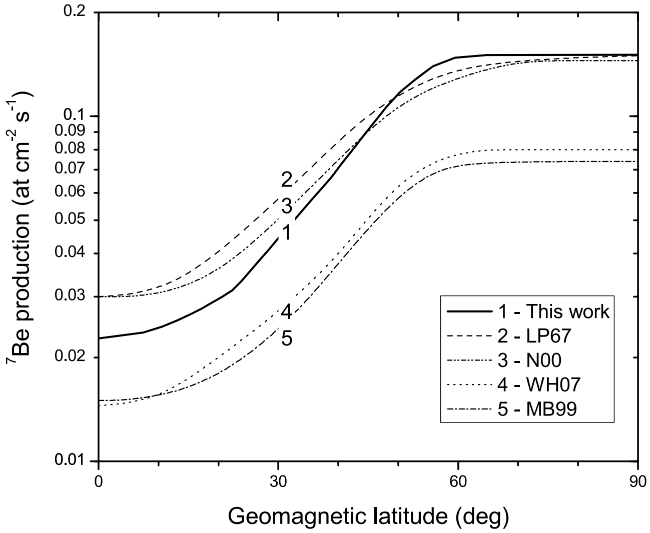

Figure 8. Column (integral over atmospheric column) production of ^{7}Be for a medium solar activity as function of geomagnetic latitude, according to different models (results for WH07 model are obtained as scaling of the ^{10}Be results), as indicated in the legend. Results are shown in log scale in order to compare the shape of curves.

during the last centuries, the estimated ^{7}Be global production was about 0.067 (at cm^{-2} s^{-1}), i.e., 8% higher, for the epoch 1955.

3. Testing the Model

3.1. Comparison With ^{7}Be Measurements

[34] Because of the wide diversity of model results (as discussed in the forthcoming subsection), we first compare our simulation results with direct measurements as the most robust test.

3.1.1. Production Rate

[35] The most direct comparison would be with measurements of the production rate of the isotope in the atmosphere. We know one such experiment [*Lal et al.*, 1960], when a sealed tank filled with oxygen target was exposed during two months (July–August 1959) at Echo Lake (Colorado) site at the atmospheric depth 685 g/cm^2. The average (corrected for decay) production rate of ^{7}Be in this oxygen tank was $9 \cdot 10^{-6}$ at [g target O]$^{-1}$ s^{-1}. Using the appropriate parameters (only oxygen target, h = 685 g/cm^2, P_c = 3 GV, $\phi \approx 1.3$ GV for July–August 1959 [*Usoskin et al.*, 2005]) we have obtained the expected production rate of $8 \cdot 10^{-6}$ at [g target O]$^{-1}$ s^{-1}. Thus, the model result agrees well with the direct measurement of ^{7}Be production rate in the troposphere.

3.1.2. Concentration in Stratospheric Air

[36] There have been numerous measurements of the ^{7}Be concentration in the atmosphere, from surface to the stratosphere. We show in Figure 9 some results of airborne measurements of the ^{7}Be concentrations compared with the model prediction for the same conditions (h, P_c and ϕ) taken individually for each measurement. The measured concentrations have been converted into the production rate assuming equilibrium between decay and production. The agreement is quite good (within 20%) in the stratosphere (values above 10^{-4} at g^{-1} s^{-1}), but a large disagreement is observed in the troposphere. Such a pattern is quite clear since the concentration of ^{7}Be is expected to be close to the equilibrium one in the stratosphere, where the isotope's residence time is longer than the decay time. In the troposphere, however, ^{7}Be is quickly washed out leading to the residence time shorter than the decay time. Accordingly, the measured concentration is different from the equilibrium one, and the difference depends on location and season [e.g., *Kulan et al.*, 2006].

[37] Thus, our model depicts a fairly good agreement with fragmentary data on stratospheric measurements of ^{7}Be concentration, assuming equilibrium conditions. This is a rough method, and a detailed comparison can be performed only taking into account realistic 3-D transport of air masses [e.g., *Koch et al.*, 1996; *Liu et al.*, 2001; *Field et al.*, 2006]. Such a comparison is beyond the scope of this study, but is planned for further work.

3.1.3. Concentration in Rain Water as Estimate for Tropospheric Production

[38] As discussed earlier, concentration of ^{7}Be measured in tropospheric air cannot give an easy estimate of the production rate. However, there are measurements of ^{7}Be concentration in rain water in different regions. Of special interest are regions with high level of precipitation, which washes out almost all isotope atoms produced in the troposphere. Particularly interesting is Indian region, with heavy rains during the monsoon season, where the wet deposition dominates [*Field et al.*, 2006]. This data is not expected to be affected by the seasonal (spring and fall) breaks of ^{7}Be-rich stratospheric air into the troposphere, because first the monsoon season does not usually overlap

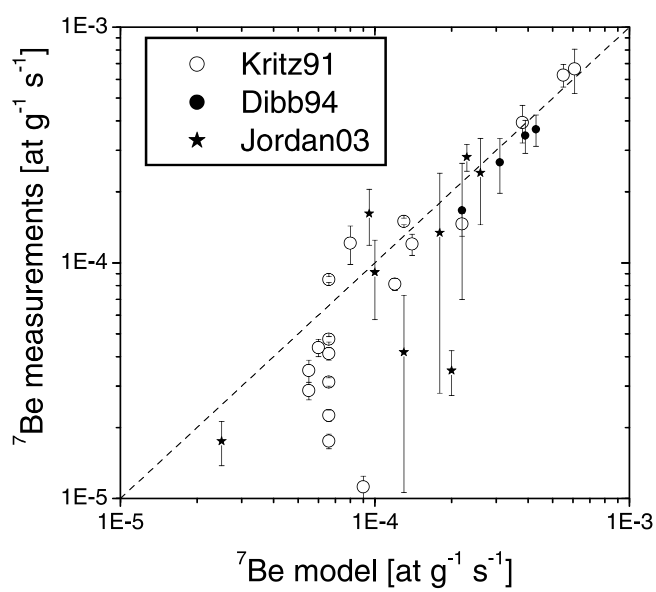

Figure 9. Scatterplot of modeled versus computed from measurements, assuming the equilibrium conditions, ^{7}Be production rate in the atmosphere. Different symbols correspond to data from *Kritz et al.* [1991], *Dibb et al.* [1994], and *Jordan et al.* [2003], as denoted in the legend.

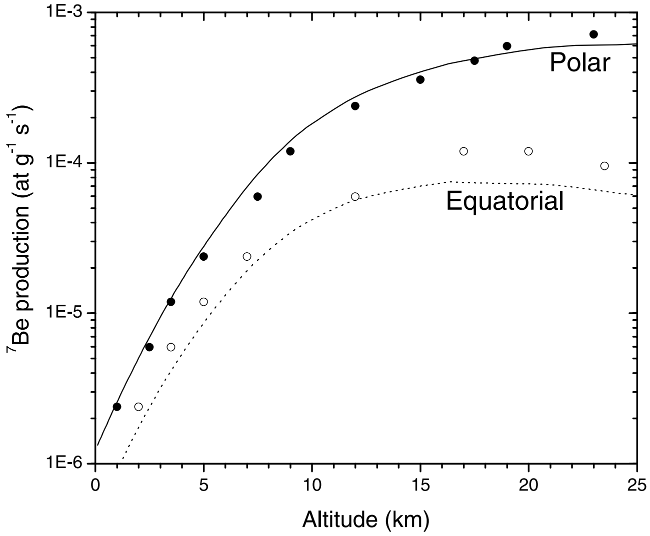

Figure 10. Altitude profile of ^{7}Be production rate for the medium solar modulation (ϕ = 0.6 GV), for geomagnetic polar and equatorial regions. Curves and symbols correspond to the results of the present and LP67 models, respectively. The present results have been converted from the atmospheric depth to the altitude using the US standard atmosphere model. The results of LP67, originally given in atoms per min per m^3 STP, have been scaled to the present units of *Y* axis.

with the seasonal breaks and second the air mixing effect is smaller in tropics compared to the midlatitudes [*Field et al.*, 2006]. Several measurements of ^{7}Be content in the rain water have been performed during the period 1956–1959 in two Indian sites: Kodaikanal ($P_c \approx 16$ GV, about 175 cm rainfall) and Bombay ($P_c \approx 15$ GV, about 100 cm rainfall) [*Rama*, 1960]. The corresponding averaged measured ^{7}Be flux was found to be $1 \cdot 10^{-2}$ and $9 \cdot 10^{-3}$ (at cm^{-2} s^{-1}), respectively. These values are close to the modeled isotope's production rate, $8.5 \cdot 10^{-3}$ (at cm^{-2} s^{-1}), computed for ϕ = 1 GV (mean modulation for 1956–1959) in the atmospheric layer 240–1030 g/cm^2 (0–11 km) for P_c = 15 GV. This assumes that all the ^{7}Be atoms produced in the troposphere are quickly, within 30 days [*Shapiro and Forbes-Resha*, 1976] (correction for decay has been applied [see *Rama*, 1960]), scavenged and eventually appear in the rain water.

[39] Thus, prediction of our model is in a reasonable agreement with the ^{7}Be fallout flux evaluated from measurements in rain water collected in India monsoon regions.

[40] Concluding this section we note that, while a direct comparison of model results with measurements is only indicative and cannot prove, in this simple form, the exactness of the model, it provides a solid ground to suggest that our model is broadly consistent with observations in the whole range: from ground level up to the stratosphere, and from equatorial to polar regions. Moreover, the fact that our model result agrees with an experiment of direct measurements of the cosmogenic ^{7}Be production rate in oxygen target (section 3.1.1) implies the correct overall normalization of the model.

3.2. Comparison With Other Models

[41] In this subsection we make an intercomparison between different models for ^{7}Be production. First we can compare the predicted total production of ^{7}Be in the atmosphere. It is noteworthy that the overall global production figures for an average solar cycle are quite controversial as given by different models (see the last row in Table 1). Our present model yields the global production rate close to those given by empirical and semi empirical models (LP67, OB79, N00) but higher than other Monte Carlo models. The present results are significantly (by a factor of 2) higher than the predictions by MB99 and WH03/07 models, and this difference is too high to be ascribed to different approaches and assumptions used. The difference is most likely related to an overall normalization rather than to modeling nuances. On the contrary, Monte Carlo models (MB99, WH03/07 and the present one) operate with pure simulations without direct fitting to the observed data, and thus are not guaranteed against a normalization error.

[42] All earlier models, except of OB79 one, provide latitudinal dependence of the column isotope production, as shown in Figure 8. One can see that the latitudinal dependence is similar for all the models, implying a similar treatment of the geomagnetic shielding. The polar-to-equatorial production ratio is about 6 for most of the models, only LP67 and N00 models yield a slightly weaker latitudinal dependence, with the polar-to-equatorial production ratio being about 5.

[43] Among earlier models only the LP67 one provides altitude profiles of ^{7}Be production, and we compare those for the polar and equatorial conditions, as shown in Figure 10. While the overall level is slightly different (compare Figure 8), shapes of the profiles are close to each other in the troposphere. Although MB99 model does not provide an altitudinal dependence of the isotope production, it estimates the relative stratospheric production as 53.5% of the entire atmospheric production, using a realistic latitude-dependent height of the tropopause. When using the same relative thickness of the troposphere as function of latitude (Figure 7 in MB99), we obtain with our model that 55% of the global ^{7}Be production can be ascribed to stratosphere. Both LP67 and N00 models yield that about 60–70% of ^{7}Be is produced in the stratosphere globally, which is consistent with the results of our model, 68%, assuming the constant heights of the tropopause at about 11 km. Note that WH03/07 model does not provide results of the relative stratospheric production.

[44] Thus, we can conclude that the present model does not contradict with earlier models in the relative variations of ^{7}Be production in both latitude and altitude. However, absolute values of the production rate differ from some earlier computations:

[45] 1. Our model results broadly agree with those by the semiempirical LP67 model, yielding however slightly lower (about 25%) global production rate.

[46] 2. Our model agrees with the analytical OB79 model in the global production similar, however the latter does not provide enough results for detailed investigation.

[47] 3. Our model predicts the global production by a factor 2 higher than the results of the MB99 model. This discrepancy is too large to be ascribed to some technical

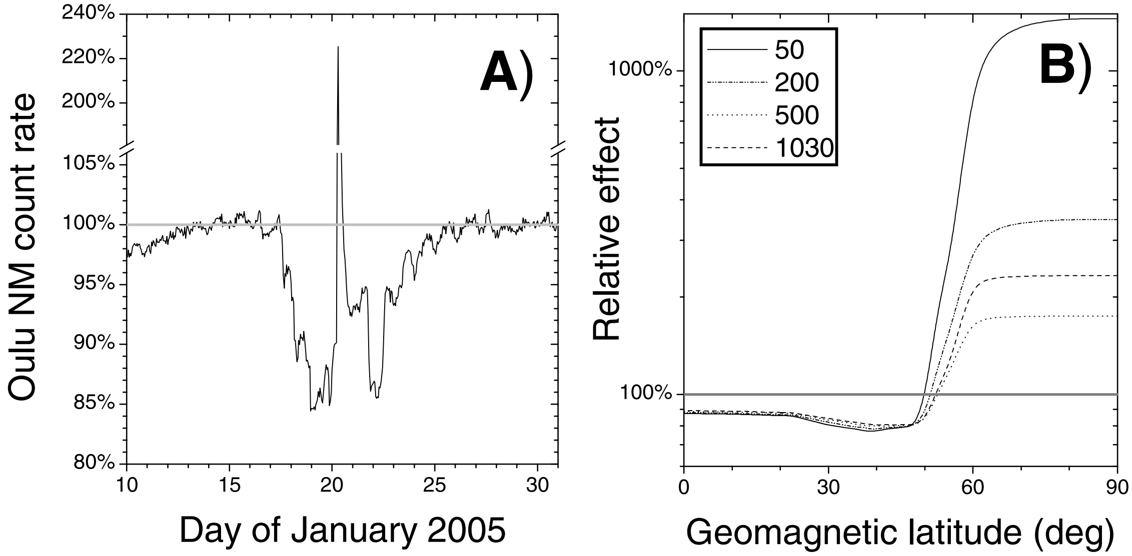

Figure 11. Combined effect of solar and galactic CR for the event of January 2005. (a) Count rate of the Oulu NM in January 2005, normalized to the period 12–17 January 2005. Note break in the *Y* axis. (b) Relative effect of solar energetic particles for the day of 20 January 2005 (see text) as a function of the atmospheric depth (different curves as denoted in the legend in g/cm^2) and geomagnetic latitude (*X* axis).

differences in the model treatment, and is most likely caused by an overall normalization.

[48] 4. Our model broadly agrees with a semiempirical N00 model, including the altitudinal profile.

[49] 5. Our model is similar to the results of a recent WH03/07 model in many respects, but predicts higher (by a factor of 2) absolute production rate. The fact that the differential column production of ^{7}Be by cosmic protons, computed by the two models, is very close to each other (see Figure 2) implies that cascade simulations were done consistently in the two models. Additionally, treatment of the geomagnetic shielding was also done mutually consistently (Figure 8). Therefore, we suppose that the difference in the total production between WH03/07 and our model can be due to the different treatment of primary cosmic rays (see Table 1) or the integration.

[50] More important is that the results of our model are in good agreement with actual measurements, including the direct measurement of ^{7}Be production rate in a special target (section 3.1.1). Because of the large diversity of the modeling results in the total production rate, we mostly rely upon comparison with measurements. Therefore, we have good reasons to believe that the overall normalization of our model is correct.

4. Effect of Solar Energetic Particles

[51] While galactic CR are always present in the Earth's environment, additional sporadic fluxes of solar energetic particles (SEPs) can occur related to solar eruptive phenomenon (solar flares or coronal mass ejections), leading to transient changes in the ^{7}Be production in the atmosphere. As an example, we consider here the effect of a severe SEP event of 20 January 2005, which was one of the strongest events ever observed. Time profile of the neutron monitor count rate for this event is shown in Figure 11a, with a clear ground level enhancement (GLE) of a few hours duration. It is important that the GLE occurred during the continuing effect of a strong Forbush decrease caused by the interplanetary shock, when the CR level was reduced by 10–15% for a week (Figure 11a). The net effect of the sequence of events is negative in the neutron monitor count rate (i.e., the long-lasting Forbush decrease overcompensates the CR increase during the transient GLE). Figure 11b shows the calculated relative effect of the studied event, which is defined as follows. First, we have computed the production of ^{7}Be by GCR during the day of 20 January 2005, when the GLE occurred, and during a quite day of 15 January, using the values of ϕ = 1.3 and 0.69 GV, respectively (calculated using the method described by *Usoskin et al.* [2005]). Next we evaluated the spectrum (daily fluence) of SEP during the day of 20 January, using the spaceborne data fitted by a power law (power index −2.15) in energy up to 0.5 GeV [*Mewaldt et al.*, 2005], and applying an exponential energy cutoff in higher energy range to fit the data from the world neutron monitor network. The resultant daily fluence

$$I = 6 \cdot 10^5 E_o^{-2.15} \exp\left(\frac{-E_o}{0.6}\right), \tag{21}$$

where E_o and I are expressed in GeV and (cm^2 sr GeV)$^{-1}$, respectively, is shown in Figure 4.

[52] Applying this spectrum to equation (19), one can evaluate the additional production of ^{7}Be due to SEPs. Let us consider the ratio of the total (GCR + SEP) production during the day of 20 January 2005 to the GCR ^{7}Be production during a quite day of 15 January 2005. This ratio (or a relative effect of the SEP event in the isotope production) is shown in Figure 11 as function of geomagnetic latitude. One can see a greatly enhanced production of ^{7}Be in the (geomagnetic) high-latitude region (geomagnetic latitude above 60°) at all altitudes. The enhancement of the

daily production was a factor of 2 at the sea level up to a factor of 15 in the stratosphere. On the contrary, the isotope production was reduced by 15–20% at lower geomagnetic latitudes, because of the transient GCR suppression (Forbush decrease) started 18 January. Therefore, a strong, almost instantaneous, "injection" of ^{7}Be isotope took place in a limited geographical area during the extreme SEP event of January 2005. Taking into account the fact that parameters (altitude, latitude and time profiles) of this "injection" can be modeled, this provides a unique opportunity to trace the atmospheric transport on both global and local scales.

5. Conclusions

[53] We have presented a new model of production of cosmogenic ^{7}Be isotope in the atmosphere. The model, based on full Monte Carlo simulation of the cosmic ray induced nucleonic cascade in the atmosphere, is able to compute 3-D (altitude and geographical location) production rate of the isotope in realistic conditions. The validity of the model has been verified by quantitative agreement with different kinds of observations, including direct measurements of ^{7}Be production rate in a dedicated experiment. The present model is in qualitative agreement with earlier models, but deviates from some of them in the absolute values.

[54] We provide a detailed recipe and a set of precalculated digital tables (Tables 2 and 3 and the auxiliary material) for the yield function. Using this "do-it-yourself" kit everyone interested can compute the ^{7}Be production for given location, altitude and the spectrum of cosmic rays, including solar energetic particles. This provides a new opportunity in studying details of the atmospheric transport, since it allows, e.g., computing the isotope production along the specific trajectory of a traced air volume.

[55] We have computed the effect of a severe solar energetic particle event of 20 January 2005 and shown that it resulted in greatly enhanced production of ^{7}Be in (geomagnetic) polar regions, accompanied by suppression in all other regions. This very unusual distribution of the isotope production pattern provides a unique opportunity to study details of the atmospheric (particularly tropospheric) circulation and transport.

[56] **Acknowledgments.** We acknowledge the support from the Academy of Finland and the Finnish Academy of Science and Letters (Vilho, Yrjö and Kalle Väisälä Foundation). We thank the CORSIKA (http://www-ik.fzk.de/corsika/) and FLUKA (http://www.fluka.org/) teams for continuous updates and improvements of their codes. We are grateful to the Department of Physical Sciences (Astronomy Division and Space Physics group) of the University of Oulu for providing us with the computing facilities for Monte Carlo calculations.

References

Alcaraz, J., et al. (2000), Helium in near Earth orbit, *Phys. Lett. B*, *494*, 193–202.

Armstrong, T. W., K. C. Chandler, and J. Barish (1973), Calculations of neutron flux spectra induced in the Earth's atmosphere by galactic cosmic rays, *J. Geophys. Res.*, *78*, 2715–2726.

Bhandari, P. A., D. Lal, and Rama (1966), Stratospheric circulation studies based on natural and artificail radioactive tracer elements, *Tellus*, *18*, 391–406.

Burger, R. A., M. S. Potgieter, and B. Heber (2000), Rigidity dependence of cosmic ray proton latitudinal gradients measured by the Ulysses spacecraft: Implications for the diffusion tensor, *J. Geophys. Res.*, *105*, 27,447–27,456.

Caballero-Lopez, R. A., and H. Moraal (2004), Limitations of the force field equation to describe cosmic ray modulation, *J. Geophys. Res.*, *109*, A01101, doi:10.1029/2003JA010098.

Clem, J. M., and L. I. Dorman (2000), Neutron monitor response functions, *Space Sci. Rev.*, *93*, 335–359, doi:10.1023/A:1026508915269.

Cooke, D. J. (1983), Geomagnetic-cutoff distribution functions for use in estimating detector response to neutrinos of atmospheric origin, *Phys. Rev. Lett.*, *51*, 320–323.

Cooke, D. J., J. E. Humble, M. A. Shea, D. F. Smart, N. Lund, I. L. Rasmussen, B. Byrnak, P. Goret, and N. Petrou (1991), On cosmic-ray cut-off terminology, *Nuovo Cimento C*, *14*, 213–234.

Dibb, J. E., L. D. Meeker, R. C. Finkel, J. R. Southon, M. W. Caffee, and L. A. Barrie (1994), Estimation of stratospheric input to the Arctic troposphere: ^{7}Be and ^{10}Be in aerosols at Alert, Canada, *J. Geophys. Res.*, *99*, 12,855–12,864.

Dorman, L. (2004), *Cosmic Rays in the Earth's Atmosphere and Underground*, Kluwer Acad., Dordrecht, Netherlands.

Fassò, A., A. Ferrari, J. Ranft, and P. Sala (2001), Fluka: Status and prospective of hadronic applications, in *Proceedings of the Monte Carlo 2000 Conference*, edited by A. Kling et al., pp. 955–960, Springer, Berlin.

Field, C. V., G. A. Schmidt, D. Koch, and C. Salyk (2006), Modeling production and climate-related impacts on ^{10}Be concentration in ice cores, *J. Geophys. Res.*, *111*, D15107, doi:10.1029/2005JD006410.

Gaisser, T. K., and T. Stanev (2004), Review of particle physics, *Phys. Lett. B*, *592*, 228–234.

Gleeson, L. J., and W. I. Axford (1968), Solar modulation of galactic cosmic rays, *Astrophys. J.*, *154*, 1011–1026.

Grieder, P. K. F. (2001), *Cosmic Rays at Earth*, Elsevier, Amsterdam.

Hatton, C. (1971), The neutron monitor, in *Progress in Elementary Particle and Cosmic Ray Physics*, vol. 10, edited by J. Wilson and S. Wouthuysen, pp. 1–100, North Holland, Amsterdam.

Heck, D., J. Knapp, J. Capdevielle, G. Schatz, and T. Thouw (1998), Corsika: A Monte Carlo code to simulate extensive air showers, *FZKA 6019*, Forschungszent. Karlsruhe, Karlsruhe, Germany.

Janni, J. F. (1982), Proton range-energy tables, 1 keV–10 GeV, energy loss, range, path length, time-of-flight, straggling, multiple scattering, and nuclear interaction probability. Part I. For 63 compounds, *At. Data Nucl. Data Tables*, *27*, 147–339.

Jordan, C. E., J. E. Dibb, and R. C. Finkel (2003), ^{10}Be/^{7}Be tracer of atmospheric transport and stratosphere-troposphere exchange, *J. Geophys. Res.*, *108*(D8), 4234, doi:10.1029/2002JD002395.

Keilhauer, B., J. Blümer, R. Engel, H. O. Klages, and M. Risse (2004), Impact of varying atmospheric profiles on extensive air shower observation: Atmospheric density and primary mass reconstruction, *Astropart. Phys.*, *22*, 249–261.

Koch, D. M., D. J. Jacob, and W. C. Graustein (1996), Vertical transport of tropospheric aerosols as indicated by ^{7}Be and ^{210}Pb in a chemical tracer model, *J. Geophys. Res.*, *101*, 18,651–18,666.

Kritz, M. A., S. W. Rosner, E. F. Danielsen, and H. B. Selkirk (1991), Air mass origins and troposphere-to-stratosphere exchange associated with mid-latitude cyclogenesis and tropopause folding inferred from Be-7 measurements, *J. Geophys. Res.*, *96*, 17,405–17,414.

Kudela, K., and P. Bobik (2004), Long-term variations of geomagnetic rigidity cutoffs, *Sol. Phys.*, *224*, 423–431.

Kulan, A., A. Aldahan, G. Possnert, and I. Vintersved (2006), Distribution of ^{7}Be in surface air of Europe, *Atmos. Environ.*, *40*, 3855–3868.

Lal, D., and B. Peters (1962), Cosmic ray produced isotopes and their application to problems in geophysics, in *Progress in Elementary Particle and Cosmic Ray Physics*, vol. 6, edited by J. Wilson and S. Wouthuysen, pp. 77–243, North Holland, Amsterdam.

Lal, D., and B. Peters (1967), Cosmic ray produced radioactivity on the Earth, in *Handbuch der Physik*, vol. 46/2, edited by K. Sittle, pp. 551–612, Springer, Berlin.

Lal, D., and H. Suess (1968), The radioactivity of the atmosphere and hydrosphere, *Annu. Rev. Nucl. Sci.*, *18*, 407–434.

Lal, D., J. R. Arnold, and M. Honda (1960), Cosmic-ray production rates of Be^7 in oxygen, and P^{32}, P^{33}, S^{35} in argon at mountain altitudes, *Phys. Rev.*, *118*, 1626–1632.

Lange, H.-J., et al. (1994), Production of residual nuclei by α-induced reactions on C, N, O, Mg, Al and Si up to 170 meV, *Appl. Radiat. Isotopes*, *46*, 93–112.

Liu, H., D. J. Jacob, I. Bey, and R. M. Yantosca (2001), Constraints from ^{210}Pb and ^{7}Be on wet deposition and transport in a global three-dimensional chemical tracer model driven by assimilated meteorological fields, *J. Geophys. Res.*, *106*, 12,109–12,128.

Masarik, J., and J. Beer (1999), Simulation of particle fluxes and cosmogenic nuclide production in the Earth's atmosphere, *J. Geophys. Res.*, *104*, 12,099–12,111.

Mewaldt, R. A., M. Looper, C. Cohen, G. Mason, D. Haggerty, M. Desai, A. Labrador, R. Leske, and J. Mazur (2005), Solar-particle energy spectra during the large events of October–November 2003 and January 2005, *Proc. Int. Cosmic Ray Conf.*, *1*, 111–114.

Nagai, H., W. Tada, and T. Kobayashi (2000), Production rates of ^{7}Be and ^{10}Be in the atmosphere, *Nucl. Instrum. Methods Phys. Res. B*, *172*, 796–801.

O'Brien, K. (1979), Secular variations in the production of cosmogenic isotopes in the Earth's atmosphere, *J. Geophys. Res.*, *84*, 423–431.

O'Brien, K. (2005), The theory of cosmic-ray and high-energy solar-particle transport in the atmosphere, in *Proceedings of the 7th International Symposium on the Natural Radiation Environment*, edited by J. McLaughlin, S. Simopoulos, and F. Steinhusler, pp. 29–44, Elsevier, Amsterdam.

O'Brien, K., A. de La Zerda Lerner, M. Shea, and D. Smart (1991), The production of cosmogenic isotopes in the Earth's atmosphere and their inventories, in *The Sun in Time*, edited by C. P. Sonett, M. S. Giampapa, and M. S. Matthews, pp. 317–342, Univ. of Ariz. Press, Tucson.

Raisbeck, G. M., F. Yiou, M. Fruneau, J. M. Loiseaux, M. Lieuvin, and J. C. Ravel (1981), Cosmogenic Be-10/Be-7 as a probe of atmospheric transport processes, *Geophys. Res. Lett.*, *8*, 1015–1018.

Rama, (1960), Investigations of the radioisotopes Be^{7}, P^{32} and S^{35} in rain water, *J. Geophys. Res.*, *65*, 3773–3776.

Shapiro, M. H., and J. L. Forbes-Resha (1976), Mean residence time of ^{7}Be-bearing aerosols in the troposphere, *J. Geophys. Res.*, *81*, 2647–2649.

Tatischeff, V., B. Kozlovsky, J. Kiener, and R. J. Murphy (2006), Delayed X- and gamma-ray line emission from solar flare radioactivity, *Astrophys. J. Suppl. Ser.*, *165*, 606–617, doi:10.1086/505112.

Usoskin, I. G., and G. A. Kovaltsov (2006), Cosmic ray induced ionization in the atmosphere: Full modeling and practical applications, *J. Geophys. Res.*, *111*, D21206, doi:10.1029/2006JD007150.

Usoskin, I. G., K. Alanko-Huotari, G. A. Kovaltsov, and K. Mursula (2005), Heliospheric modulation of cosmic rays: Monthly reconstruction for 1951–2004, *J. Geophys. Res.*, *110*, A12108, doi:10.1029/2005JA011250.

Webber, W. R., and P. R. Higbie (2003), Production of cosmogenic Be nuclei in the Earth's atmosphere by cosmic rays: Its dependence on solar modulation and the interstellar cosmic ray spectrum, *J. Geophys. Res.*, *108*(A9), 1355, doi:10.1029/2003JA009863.

Webber, W. R., P. R. Higbie, and K. G. McCracken (2007), Production of the cosmogenic isotopes ^{3}H, ^{7}Be, ^{10}Be, and ^{36}Cl in the Earth's atmosphere by solar and galactic cosmic rays, *J. Geophys. Res.*, *112*, A10106, doi:10.1029/2007JA012499.

G. A. Kovaltsov, Ioffe Physical-Technical Institute, Politekhnicheskaya 26, RU-194021 St. Petersburg, Russia.

I. G. Usoskin, Oulu Unit, Sodankylä Geophysical Observatory, University of Oulu, P.O. Box 3000, FIN-90014 Oulu, Finland. (ilya.usoskin@oulu.fi)